Weather and Climate Extremes 39 (2023) 100546

Contents lists available at ScienceDirect

Weather and Climate Extremes

journal homepage: www.elsevier.com/locate/wace

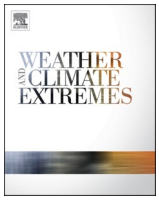

Attribution of the 2015 drought in Marathwada, India from a multivariate perspective

Mariam Zachariah [a,d], Savitri Kumari [b], Arpita Mondal [a,b,*], Karsten Haustein [c], Friederike E. L. Otto [d]

[a] Department of Civil Engineering, Indian Institute of Technology Bombay, Mumbai, India
[b] Interdisciplinary Program in Climate Studies, Indian Institute of Technology Bombay, Mumbai, India
[c] Institute for Meteorology, Universität Leipzig, Leipzig, Germany
[d] Grantham Institute, Imperial College, London, United Kingdom

ARTICLE INFO

Keywords:
Probabilistic event attribution
Drought
Climate change
Multivariate return period
Copula

ABSTRACT

The agricultural region of Marathwada in India incurred significant loss of crops and lives during the summer of 2015, which was characterised by persistent hot and dry conditions. We use observations and large ensembles of regional climate model simulations to understand and attribute this joint occurrence of deficient rainfall and high temperature in a novel, multivariate framework. Highly unlikely in a world without anthropogenic climate change (1-in-256 year), the event is found to be frequent (1-in-38 year) in the actual world. Thus, the risk of this event is found to be atleast quintupled due to anthropogenic factors, implying that the 2015 event is more likely due to anthropogenic climate change. Interestingly, the 2015 dry event is not unprecedented (~1-in-15 year) based on observed records and for either of the model scenarios, suggesting that risk assessments based on rainfall alone may not be enough to reconcile the observed impacts. Further, such compound drought events are projected to become even more frequent under future end-of-the-century warming targets of 1.5 °C and 2 °C above pre-industrial levels, with expected doubling and tripling of the probability of the 2015 hot-dry conditions, respectively. Our findings highlight the role of human-induced warming on increased incidences of compound extreme events, thereby warranting adaptation strategies that aim at alleviating associated risks.

1. Introduction

Rainfall deficit is the principal driver of droughts; however, a compounding role of rising temperatures in prolonging and/or intensifying such extremes is increasingly reported from different parts of the world (Diffenbaugh et al., 2015; Mishra et al., 2020; Nicholls, 2004; Sarhadi et al., 2018; Zscheischler et al., 2018). Such compounded extremes are expected to have more disastrous impacts than their univariate counterparts (Hao et al., 2018). For example, higher regional temperatures during droughts can exacerbate heatwaves (AghaKouchak et al., 2014; Chiang et al., 2018; Panda et al., 2017; Sharma and Mujumdar, 2017). Furthermore, such conditions can also be detrimental to crop growth due to increased evapotranspiration rates (Goyal 2004) and reduction in soil moisture (Kumar et al., 2017; Mishra et al. 2014, 2019), thereby having important implications for the agricultural economy of India (Mishra et al., 2019, 2020).

In 2015, India experienced extensive drought conditions, with the rainfall deficit accompanied by anomalously high temperatures in many parts of the country (Ghatak et al., 2017). Impacts included marked increases in crop loss and farmer suicides, both of which have been shown to be sensitive to rainfall deficits and rising temperatures due to climate change (Carleton, 2017; Parida et al., 2018). The effects were particularly catastrophic for the drought-prone, semi-arid, agricultural region of Marathwada in the state of Maharashtra (Fig. 1(a)). The total insurance amount claimed under crop loss in the state was estimated at $594.5 million (Jain 2016). Maharashtra also recorded the highest number of suicides in the farming sector at 4 291 deaths (NCRB, 2016), with most of these deaths reported from the Marathwada and Vidarbha sub-divisions (Gangan 2016; Vyas 2016).

Existing studies differ in opinion as to whether the severe impacts of the 2015 drought event were primarily caused by local water management issues (Fernandes, 2016; Kulkarni et al., 2016; Seetharaman, 2017), or a manifestation of climate change (Deulgaonkar and Joshi 2016; Ghatge 2016). However, these studies are mostly conjectural and

* Corresponding author. Department of Civil Engineering Indian Institute of Technology Bombay Powai, Mumbai, 400076, India.
E-mail address: marpita@civil.iitb.ac.in (A. Mondal).

https://doi.org/10.1016/j.wace.2022.100546
Received 30 May 2022; Received in revised form 22 October 2022; Accepted 27 December 2022
Available online 30 December 2022

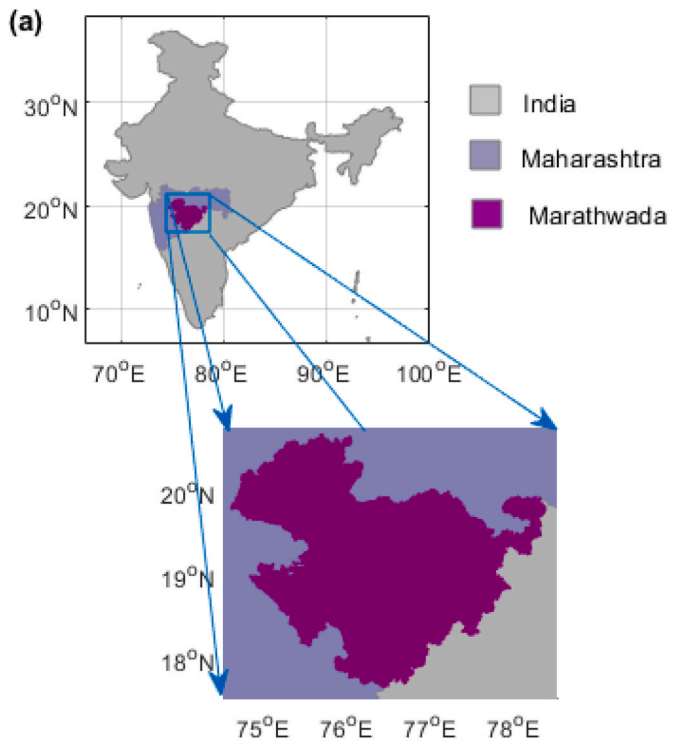

Fig. 1. Map of India showing the Marathwada region. The blue box (17.5°N-20.5°N, 74.5°E–78.5°E) is the representative domain for Marathwada. (For interpretation of the references to colour in this figure legend, the reader is referred to the Web version of this article.)

based on preliminary analysis using observed data alone. The Probabilistic Event Attribution (PEA) framework (Otto et al., & Allen, 2012; Pall et al., 2011; Stone and Allen, 2005; Stott et al., 2004) presents a formal, more robust means of investigating the role of anthropogenic climate change on individual extreme events such as droughts (Lott et al., 2013; Philip et al., 2018; Uhe et al., 2018). Studies on application of PEA to events in India are rather limited in number (Kumari et al., 2019; van Oldenborgh et al., 2018; Wehner et al., 2016). In particular, there are no studies to date that have attempted an attribution analysis on drought events in India. The vulnerability of agrarian communities to droughts, particularly in the semi-arid regions (D. Singh et al., 2014) necessitates the analysis of such events in a PEA framework, as the findings can have implications for a more inclusive decision-making that weigh in the role of anthropogenic climate change (Thompson and Otto 2015).

The 2015 southwest monsoon over India was characterized by weak monsoon circulations due to canonical El-Niño conditions over the Pacific Ocean, and short-lived depressions with short tracks that limited the rainfall to localized downpours (Mujumdar et al., 2015). Consequently, the monsoons failed to produce widespread rainfall over the core monsoon zone, thus resulting in a 14% rainfall departure across India, and a more severe 40% deficit in Marathwada (Purohit and Kaur 2017). Most parts of the country including Marathwada were also characterized by above-average temperature towards the end of the pre-monsoon (MAM) season and for the major part of the monsoon (JJAS) season (IMD, 2016). Ghatak et al. (2017) identified that local land-atmosphere feedbacks due to dry soils in the pre-monsoon period played a significant role in compounding the 2015 drought in India, by raising the temperatures that led to the heatwave conditions in parts of the country. Prior to the onset of the monsoons, clear skies and dry atmospheric conditions led to elevated incoming shortwave radiation that resulted in land surface warming (Ratnam et al., 2016). This caused soil moisture deficits to develop, leading to drying of the surface, which in turn caused the hot conditions to persist into the monsoon months due to the sensible heat flux associated with drying. The study (Ghatak et al., 2017) also highlighted that the semi-arid, agricultural landscape of North and Central India that includes Marathwada is prone to heat extremes under dry conditions, as also confirmed by later studies (Mishra et al., 2020; Sharma and Mujumdar 2017).

Kulkarni et al. (2016) examined long-term rainfall records and found that the deficient JJAS rainfall in 2015 over Marathwada was within the observed variability over Marathwada, thus challenging the role of climate change. The authors also argued that the event should have been expected given that El-Niño was predicted for the season. However, using observed records of rainfall and temperature and climate model simulations that capture the coupling between El-Niño and the Indian Summer Monsoon Rainfall (ISMR), Mishra et al. (2020) showed that hot and dry extremes over India, are found to be made more frequent due to greenhouse gas warming. Therefore, a multivariate framework that account for the interdependencies between rainfall and temperature (Chiang et al., 2021; Hao and Singh, 2020) is necessary for a realistic attribution of the drought characteristics in the region, as opposed to standard approaches based on rainfall alone that may underestimate the risk (AghaKouchak et al., 2014; Zscheischler and Seneviratne, 2017).

In this study, we present a first-of-its-kind attribution study on the compounded drought of 2015 in Marathwada, India. We use a copula-based multivariate framework for characterizing the event. Copulas have the distinct advantage of combining meteorological information about the event based on their dependency structure (e.g., AghaKouchak et al., 2014; Hao et al., 2018), and require no assumptions about the marginal distributions of these variables or their functional relationship with the event (e.g., Roberts et al., 2013).While the PEA framework has been successfully applied to several extreme weather events globally, to the best of our knowledge, this study presents the first application of PEA analysis from a multivariate perspective. We compute the joint return period of deficient rainfall and anomalously high temperature based on both observations, and large ensembles of regional climate model simulations for multiple scenarios: Actual-the (factual) world under current warming conditions, Natural-a counterfactual world that might have been without anthropogenic influence, and two future warming targets that limit global warming to 1.5 and 2 °C above pre-industrial levels at the end of the 21st century (UNFCCC United Nations Framework Convention on Climate Change, 2016). Finally, we compare the event probability in the different scenarios, for deducing the evolution of the event's recurrence characteristics from past through present, to future warming projections.

2. Data and model simulations

2.1. Observed data

Gridded datasets of daily rainfall and temperature from India Meteorological Department (IMD; available at http://www.imdpune.gov.in/Clim_Pred_LRF_New/Grided_Data_Download.html), for the period 1951–2015 (Pai et al., 2014; Srivastava et al., 2009) constitute the observed data. While rainfall is available at 0.25° × 0.25° spatial resolution, interpolated (Shepard, 1968) from 6 995 rain gauge station records across India (Pai et al., 2014), temperature is available at a relatively coarser resolution of 1° × 1°, interpolated from records in 395 stations across the country (New et al., 2000; Shepard, 1984; Willmott et al., 1985). These products have been widely used in hydrometeorological studies (e.g., Bhavani et al., 2017; Chaudhary et al., 2017; Duncan et al., 2016; Mazdiyasni et al., 2017; Soora et al., 2013; Vinnarasi and Dhanya, 2016). The gridded data are spatially averaged over Marathwada (17.5°N – 20.5°N, 74.5°E – 78.5°E; red box in Fig. 1(a)).

2.2. Model simulations-weather@home

The climate model simulations consist of large ensembles of the factual and counterfactual worlds from the volunteer-distributed computing project, weather@home (Guillod et al., 2017; Massey

et al., 2015). Using large ensembles significantly improves the confidence of the results, thus enabling a statistically robust attribution of the weather/climate extreme event (Sippel and Otto, 2014). The simulations are generated at ~50 km resolution, centered over South Asia (https://www.climateprediction.net/weatherathome/regions/) by the regional climate model (RCM) Hadley Centre Regional Climate Model version 3P (HadRM3P). This RCM is nested in the atmosphere-only global climate model Hadley Centre Atmospheric Model *version* 3P (HadAM3P), and is driven by observed sea surface temperatures (SST) and sea ice concentration from Operational Sea Surface Temperature and Sea Ice Analysis (OSTIA) dataset (Donlon et al., 2012).

The model scenarios consist of 200 realizations of the simulated climate variables under the factual (Actual) and two counterfactual (Natural and GHG-only) scenarios, for the period 1986–2015. The Natural scenario envisages a world without anthropogenic emissions while the GHG scenario represents a world with no anthropogenic aerosols. Further, 100 shorter realizations (10 years that correspond to the 2006–2015 period) of these variables for two projected future scenarios (1.5 °C warmer and 2 °C warmer) are also used for a prognosis of compound drought risks under future climate change. These scenarios, post the Paris Accord (UNFCCC United Nations Framework Convention on Climate Change, 2016), presume 1.5 °C and 2 °C global warming above pre-industrial levels by the end of 21st century and are intended for assessments under Half a degree Additional warming, Prognosis and Project Impacts (HAPPI) framework (Mitchell et al., 2017). More details about the HadRM3P-HadAM3P nested model setup and construction of the different scenarios considered in the study are provided in Supplementary Section S1.

3. Methodology

Fig. 2 shows the schematic of the methodology adopted in this study for attributing the observed hot and dry conditions that characterized the 2015 drought event in Marathwada, hereafter called as *the 2015 hot and dry event*. Firstly, an event definition that reflects the extremity of the impacts in the region is arrived at, based on insights available for the region in general, and specific to the event (discussed in Section 4.1). In the next step, the climate model is evaluated for assessing its suitability for simulating the rainfall and temperature features in Marathwada (discussed in Section 4.2). Finally, the return period of the 2015 hot and dry event under the factual and counterfactual scenarios and the relative probabilities are calculated, for assessing the change in likelihood of the event under the different scenarios.

3.1. Joint probability distributions and multivariate return period

The joint probability distributions of rainfall and temperature from which the return periods of the 2015 hot and dry event are estimated for different scenarios, are derived using copulas (e.g., Pandey et al., 2018; Wazneh et al., 2020). Copulas are statistical functions that map the marginal cumulative distribution functions (CDFs) of multiple variables - rainfall and temperature in this case, to their joint CDFs through a function that models the dependence between the variables. The best-fitting marginal probability distributions for reverse rainfall series ($X = 0 - X'$, where the actual rainfall series is X'; AghaKouchak et al., 2014; Serinaldi, 2016) and temperature (Y) are selected based on goodness-of-fit measures, from among a candidate set of parametric models, namely, Log-normal, Normal, Gamma and Weibull

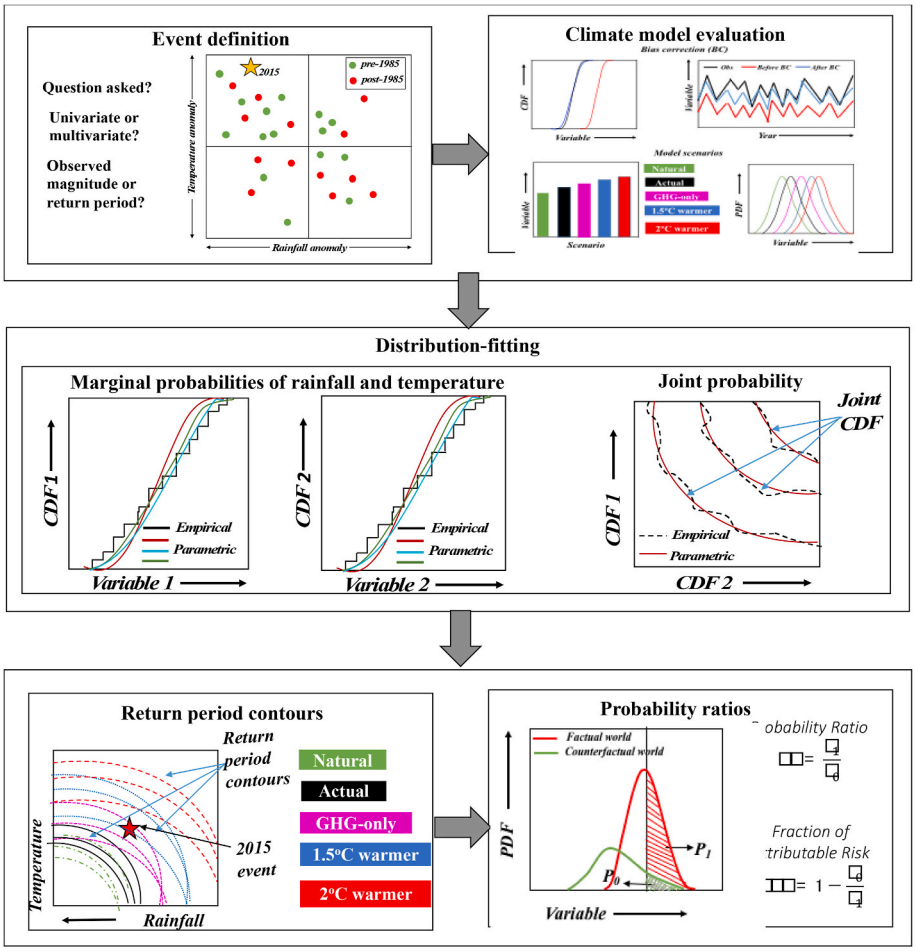

Fig. 2. Illustration of the multivariate attribution framework.

distributions. The parameters of the distributions are estimated using the maximum likelihood method (Myung 2003). Three metrics are used for evaluating the goodness-of-fit of the candidate distributions- Mean Squared Error (MSE), Akaike Information Criterion (AIC; Akaike, 1386; Bozdogan, 2000) and Kolmogrov-Smirnov (K–S) distance (Kolmogorov 1933; Massey 1951; Smirnov 1948). The empirical CDF distributions of the variables required for calculating the goodness-of-fits are estimated from the Gringorten plotting position formula (Gringorten 1963). For each of the variables, the distribution corresponding to the lowest estimates for these metrics is chosen as the best-fitting probability distribution.

Similarly, the joint probability distribution of X and Y is modelled using an appropriate copula, chosen from among different copula families by comparing with the empirical bivariate CDF estimates from a modified version of the Gringorten formula (Yue 2001). The copulas considered in this study are the Gaussian, Frank and Students-t copulas (AghaKouchak et al., 2014; Serinaldi 2016). The best-fitting copula is chosen as the one which gives the lowest estimates for MSE, AIC and K–S distance. These joint probabilities are then used to compute the joint return period of the 2015 hot-dry event, as follows (AghaKouchak et al., 2014):

i. From the best-fitting cumulative distribution functions (CDFs) F_X and F_Y that respectively model X and Y, we obtain paired CDF estimates (u,v), where $u = F_X(x) = \Pr(X \le x)$ and $v = F_Y(y) = \Pr(Y \le y)$, for all $(x,y) \in (X,Y)$.
ii. The joint cumulative distribution function F_{XY} are estimated from the marginals F_X and F_Y, using copulas (Nelsen 2006), as:

$$F_{XY}(x,y) = \Pr(X \le x, Y \le y) = C(u,v) \quad (1)$$

iii. The joint survival function $\overline{F}_{XY}(x,y) = \Pr(X > x, Y > y)$ is estimated from the marginal survival functions $\overline{F}_X(x) = 1-u$ and $\overline{F}_Y = 1-v$, using survival copula (Nelsen 2006), as:

$$\overline{F}_{XY}(x,y) = \widehat{C}(\overline{F}_X(x), \overline{F}_Y(y)) = 1-u-v+C(u,v) \quad (2)$$

iv. For any $(X,Y)\varepsilon R^2$, there exists a survival critical layer (or isoline) $\mathscr{L}_p^{\overline{F}}$ on which a subset $(x,y) \in (X,Y)$ shares the same probability p. i.e.,

$$\mathscr{L}_p^{\overline{F}} = \{(x,y)\varepsilon R^2 : \overline{F}(x,y) = p\} \quad (3)$$

v. The corresponding survival return period (T)is given by $T = \frac{1}{p}$. This information is utilized for plotting the isolines (contours) corresponding to a subset of return periods.

3.2. Assessing change in event probability to climate change

Probability ratio ($PR = P_1/P_o$) is calculated from the probabilities of the event in the factual (P_1) and counterfactual scenarios (P_0) for quantifying the change in likelihood of the 2015 event due to observed and expected future climate change. The probability ratio $PR \in (0,\infty)$ gives the factor by which the event in the factual world is more ($PR < 1$) or less ($PR > 1$) likely as compared to the world that might have been. Therefore, $PR = 1$ indicates that the event is equally likely in the counterfactual and factual worlds. We use the calibrated language proposed by Lewis et al. (2019) for communicating the attribution results from this study. Accordingly, the likelihood category (see Table 1 in Lewis et al. (2019)) of the event is reported, based on a lower confidence bound, which in this case is the 10th percentile value of PR associated with the 90% confidence interval.

Table 1
The return periods and probability ratios (PR), at a glance, for the different observed time periods and model scenarios.

For the 2015 hot-dry event						
Observations			Model simulations			
Period/Scenario	Return period	Range	Pair	PR	Best estimate	Likelihood
pre-1985	570	170–6 500	post-1985/pre-1985	0.57	5	
post-1985	110	50–470				
Climatology	100	90–110				
Natural	262	216–330	Actual/Natural	5.3	6.5	*More likely*
Actual	38	33–44	Actual/GHG-only	0.5	0.6	*Exceptionally less likely*
GHG-only	22	20–25	1.5 °C warmer/Actual	2.1	2.6	*More likely*
1.5 °C warmer	15	13–17	2 °C warmer/Actual	2.8	3.4	*More likely*
2 °C warmer	12	10–14	2 °C warmer/1.5 °C warmer	1	1.3	*Very much less likely*
For the 2015 dry event						
Observations			**Model simulations**			
Period/Scenario	***Return period***	***Range***	***Pair***	***PR***	***Best estimate***	***Likelihood***
pre-1985	16	9–45	post-1985/pre-1985	0.5	1.1	
post-1985	15	11–28				
Climatology	14	12–15				
Natural	17	16–19	Actual/Natural	1	1.2	*Very much less likely*
Actual	15	13–17	Actual/GHG-only	1.3	1.5	*Did not alter*
GHG-only	22	19–24	1.5 °C warmer/Actual	0.8	1	*Exceptionally less likely*
1.5 °C warmer	15	13–17	2 °C warmer/Actual	1.1	1.3	*Less likely*
2 °C warmer	12	10–14	2 °C warmer/1.5 °C warmer	1	1.3	*Very much less likely*
For the 2015 hot event						
Observations			**Model simulations**			
Period/Scenario	***Return period***	***Range***	***Pair***	***PR***	***Best estimate***	***Likelihood***
pre-1985	108	46–555	post-1985/pre-1985	2.1	6.8	
post-1985	16	10–36				
Climatology	10	9–11				
Natural	55	50–63	Actual/Natural	11.4	12.9	*Very much more likely*
Actual	4	3–5	Actual/GHG-only	0.3	0.32	*Exceptionally less likely*
GHG-only	1	1–3	1.5 °C warmer/Actual	3	3.2	*More likely*
1.5 °C warmer	1	1–3	2 °C warmer/Actual	3.9	4.1	*More likely*
2 °C warmer	1	1–3	2 °C warmer/1.5 °C warmer	1.2	1.3	*Did not alter*

4. Results and discussions

4.1. Event definition

For performing robust attribution analyses, it is necessary to adopt a definition that best reflects the event extremetity as well as its impacts, and over a homogeneous region (Philip et al., 2020). Based on country-wide averages, Mishra et al. (2020) showed that concurrent hot and dry monsoons in India including the one in the year 2015, were associated with shortfall in crop yields. Therefore, the feasibility of adopting a similar definition for the 2015 drought event in Marathwada is explored. To this end, we define the 2015 hot and dry event by the cumulative rainfall and average temperature in the JJAS season, spatially-averaged over the study region (Fig. 1(a)). This is a justified choice, given that Marathwada is homogeneous in climate and topography (Kelkar and Sreejith 2020; Fig. 1(a)), and the impact during the 2015 event was primarily agrarian (see Section 1).

Fig. 3(a–b) shows the observed time series of JJAS cumulative rainfall and average temperature for Marathwada, for the period 1951–2015. The rainfall shows decreasing trends, both in this period, and the recent 1986–2015 period. However, the observed decrease in the rainfall post-1985 is not significant at the 90% confidence level (Fig. 3(a)). ISMR is fraught with significant internal variability and sensitivity to large-scale teleconnections (Kripalani and Kulkarni, 1997; K. K. Kumar et al., 2006) which partly explains the lack of statistically significant trends for shorter spans. Temperature, on the other hand, shows higher rates of warming during the post-1985 period, as compared to the long-term trend, both significant at 90% confidence level (Fig. 3(b)). This observation is consistent with other studies that report higher rates of warming globally and over India after 1980 (e.g., Hansen et al., 2012; Panda et al., 2017).

Fig. 3(c–d) shows the ranked plots of cumulative monsoon season (JJAS) rainfall and average JJAS mean temperatures in Marathwada for 65 years, from 1951 to 2015. The temperature in 2015 is the third highest, after 2009 and 1995 (Fig. 3(c)). The rainfall deficit is not as rare, with similar rainfall amounts observed in 1952, 1971, 1972 and 1984 (Fig. 3(d)).

For the rest of the analysis, the observed data is split at 1985 to create pseudo-counterfactual (1951–1985 or pre-1985) and factual (1986–2015 or post-1985) datasets (e.g. Sippel and Otto, 2014). Over India, the post-1980 period is found to show increased rates of warming and drying (Panda et al., 2017; D. Singh et al., 2014) due to the rapid warming of western Indian Ocean as compared to the sub-continent (Roxy et al., 2015), rising regional anthropogenic aerosol emissions (Bollasina et al., 2011) and changes in land use/land cover characteristics (Paul et al., 2016), all of which can be linked to increased human activities. The split point is categorically chosen as the year 1985 to also allow direct comparisons with the weather@home model climatology period of 1986–2015 (details in Section 4.2).

The standardized anomalies of JJAS rainfall and temperatures in Marathwada are shown in Fig. 3(e). The anomaly scatter features a negative slope, suggesting that the droughts in the region concur with anomalously high seasonal temperature. The second quadrant that is characterized by hot and dry conditions has a higher concentration of events from post-1985 (43%), as compared to 33% of the events from pre-1985 period. The years with concurrent country-wide hot and dry extremes that significantly impacted crop productivity (Mishra et al., 2020), are highlighted in yellow. It is interesting to note that all of these years are characterized by concurrent hot and dry conditions in Marathwada, as well. Therefore, the 2015 hot and dry event is defined by the jointly observed, spatial-averaged cumulative rainfall and mean temperature for the 2015 JJAS season.

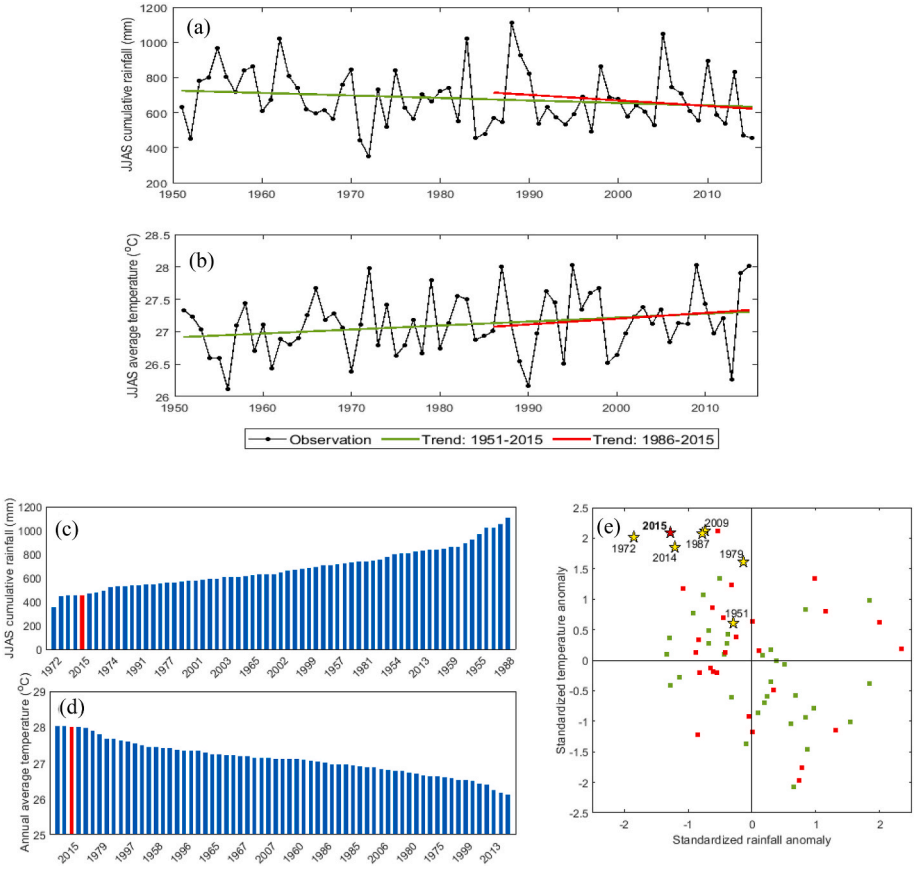

Fig. 3. **(a)** Time series of JJAS cumulative rainfall from 1951 to 2015. The linear trends for 1951–2015 (green) and 1985–2015 (red) are superimposed on the time series. **(b)** *same as* (a), for JJAS mean temperature **(c)** Ranked JJAS cumulative rainfall and **(d)** JJAS mean temperature, from 1901 to 2015. Red bars denote the corresponding values for 2015. The rainfall (temperature) lie in the lower (upper) 10th percentile of the observed records. **(e)** Standardized anomalies of JJAS rainfall and JJAS average temperature, w.r.t the 1960–1990 mean. The green dots and the red dots are standardized annual anomalies, pre-1985 (1901–1985) and post-1985 (1986–2015), respectively. The 2015 event is denoted by the red pentagram. Previous historical drought events in 2014, 1984, 1972 and 1920, are shown by blue, green, yellow and cyan pentagrams respectively. (For interpretation of the references to colour in this figure legend, the reader is referred to the Web version of this article.)

4.2. Climate model evaluation

The 30-year period from 1986 to 2015 is chosen as the reference climatology for evaluating the climate model simulations against observed data. The observed global average warming over this period is unbiased by short-term variability (Allen et al., 2018), thus making it suitable for studies seeking to discern anthropogenic climate change effects. Further, as explained in Section 4.1, this period is characterized by increased warming and drying over the Indian sub-continent, due to increased anthropogenic activity.

Fig. 4 shows the performance of the regional model HadRM3P in simulating the southwest (JJAS) monsoon (Fig. 4(a–b)) and the JJAS seasonal average temperature (Fig. 4(c–d)) over the Indian sub-continent. In contrast to rainfall (Fig. 4(a–b)), temperature is a relatively smooth variable with a large degree of randomness and less-noisy patterns driven by the topology. Therefore, apart from mountainous regions being noticeably cooler than low-lying areas, most of the country including Marathwada shows no discernible spatial patterns in observed and model-based temperatures (Fig. 4(c–d)). Overall, the observations and the model simulations are found to match well for both

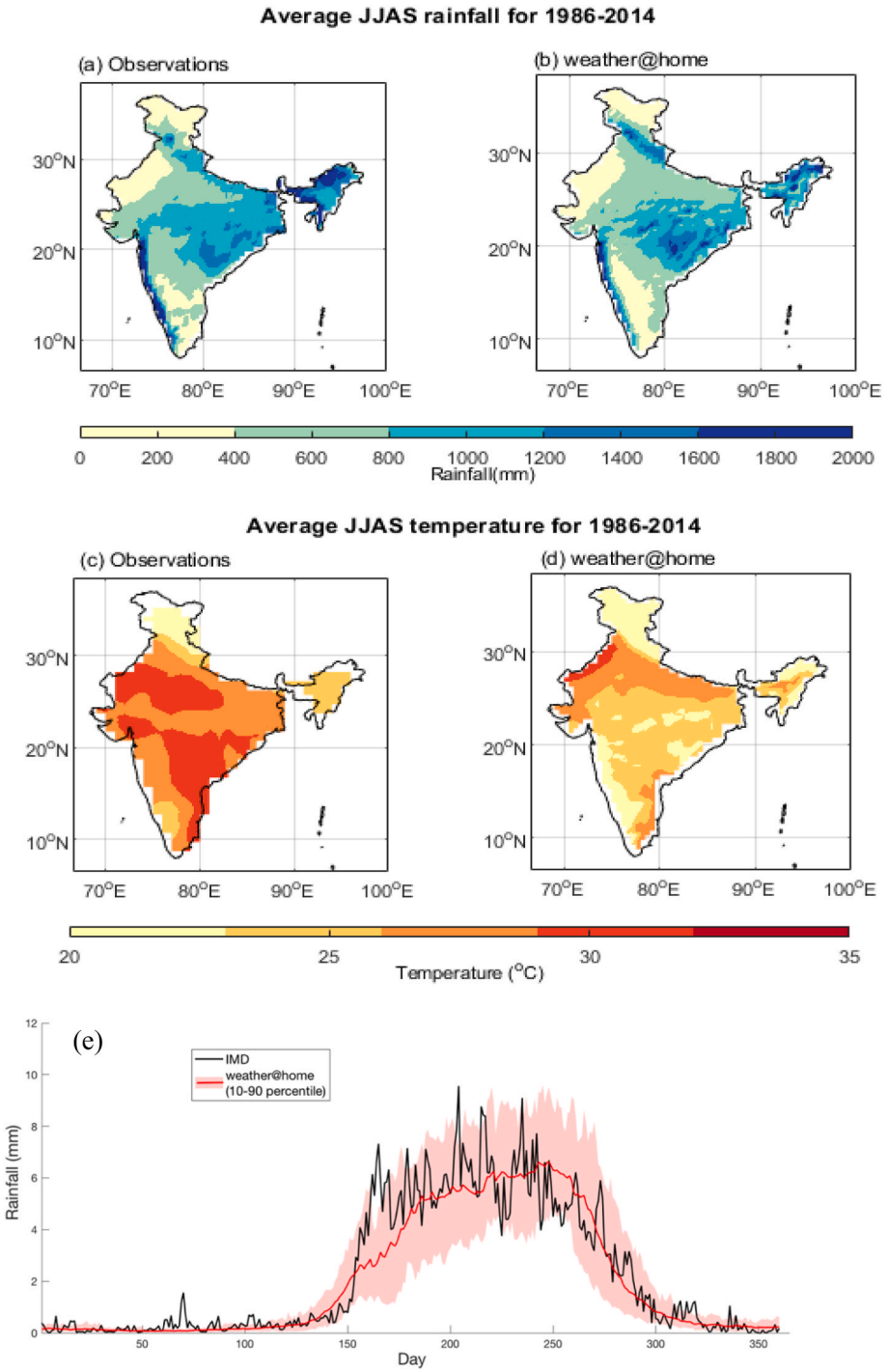

Fig. 4. JJAS cumulative rainfall averaged over the period 1986–2014 for **(a)** observations and, **(b)** weather@home simulations. Seasonal (JJAS) average temperature, averaged over 1986–2014 for **(c)** observations and, **(d)** weather@home simulations. The Pearson spatial correlation between the observed and model simulated averages of rainfall and temperature are 0.74 and 0.83, respectively, and both significant at 5% significance level (s.l).

rainfall and temperature, correlated at 0.74 and 0.83, respectively.

The model is also found to simulate the daily monsoon cycle in the region reasonably well, as shown in Fig. 4(e). However, unlike rainfall, the temperature is discernibly underestimated by the model (Fig. 4(d)). Therefore, for the study area, the monthly cumulative rainfall and average temperature estimated from the model simulations are corrected against observed records for removing systematic biases, by using a multivariate bias correction approach (MBC; Cannon, 2016). MBC is a multivariate analog of univariate quantile mapping (Li et al., 2010), and iteratively corrects the Pearson correlation between the variables along with the marginal distributions, so as to minimize the maximum absolute error between the observed data and the model simulations (Cannon 2016). The MBC approach has wide applications in climate model evaluations (e.g., D. Li et al., 2020; Tam et al., 2019) and impact assessments (Galmarini et al., 2019; J. Wu et al., 2021).

Fig. 5 shows the monthly and seasonal characteristics of the area-averaged ensemble mean of rainfall and temperature over Marathwada, along with the respective 90% envelope, before and after bias correction. Post bias correction, the monthly climatologies of the model simulated variables are seen to move closer to those of the observations, as shown in Fig. 5(a) and (c) for rainfall and temperature, respectively. The observed rainfall and temperature magnitudes are found to fall within the model envelope after bias correction. The model-averaged time-series of the cumulative rainfall (Fig. 5(b)) and the average temperature estimates (Fig. 5(d)), both aggregated over JJAS season, are also found to match well with the observed data, with statistically significant correlation coefficients of 0.434 and 0.517, respectively. The close agreement in the spatiotemporal characteristics of rainfall and temperature, between observed records and model simulations, allows an overall rating of *medium confidence* (Lewis et al., 2019) for the attribution results reported in this study.

For judicious comparison, the 10-year period from 2006 to 2015 that is common to all scenarios (Table S1) is adopted as the reference period for the model-based assessments in this study. Fig. 6 shows the decadal (2006–2015) mean of the bias corrected JJAS cumulative rainfall and average JJAS temperature over Marathwada under the different climate model scenarios (Fig. 6(a–b)), along with their respective probability distributions (Fig. 6(c–d)). It is observed that there is no discernible shifts in the seasonal rainfall among the different scenarios, although the seasonal average temperature is found to consistently shift to hotter regimes under human influence (Actual), in the hypothetical absence of aerosols (GHG-only), and future warming (1.5 °C warmer and 2 °C warmer). The closeness in the rainfall climatology between the factual and counterfactual scenarios is to be expected, on account of the observed and projected disparities in the rainfall distribution patterns and the spatial rainfall trends in India, even as Indian Summer Monsoon Rainfall (ISMR) is expected to increase under future warming (Ghosh et al., 2016; Guhathakurta and Rajeevan, 2008; Preethi et al., 2019). The increase in ISMR is expected to contribute primarily to the Himalaya region, the northeast of the Bay of Bengal and the west coast of India (Katzenberger et al., 2021), partially explaining the smaller increase (2%) in rainfall under future warming in Marathwada, that is situated on the rain shadow area of the Western Ghats.

4.3. Fitting marginal and joint distributions

The probability density function (PDF) and CDF plots from the candidate probability distributions (Section 3.1), when fitted to the observed JJAS rainfall (Fig. 5(b)) and temperature (Fig. 5(d)) for the period 1951–2015 are shown in Fig. 7(a–b) and Fig. 7(c and d) respectively. Table S2(a) shows the goodness-of-fit of each of these distributions based on KS-distance, MSE and AIC. The Log-normal distribution is found to be the best-fit distribution for both rainfall and temperature. The goodness-of-fit statistics of joint probability distributions by fitting the rainfall-temperature CDF pairs with the candidate copulas (Section 3.1) are given in Table S2(b). From these statistics and from visual inspection (Fig. 7(e–f); e.g., Cong and Brady, 2012), Frank copula is found to be the best-fit copula for modelling the joint probability of rainfall and temperature.

4.4. Multivariate return periods and probability ratios for the 2015 hot and dry event

Fig. 8(a) shows the return period contours of concurrent hot and dry

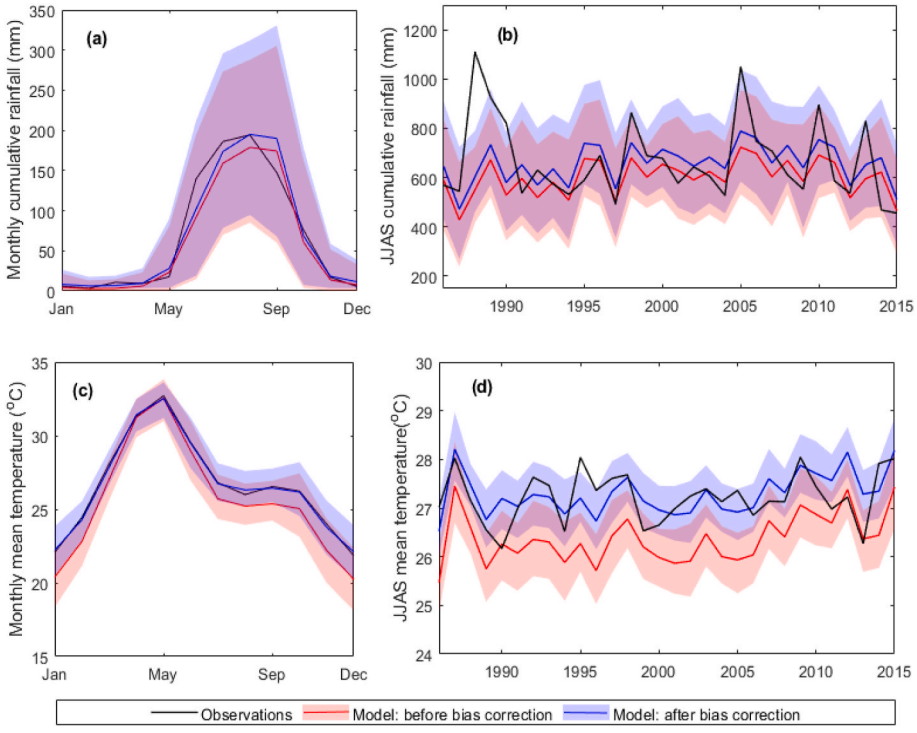

Fig. 5. (a) Monthly climatology of rainfall in the Marathwada region w.r.t. 1986–2015 period. **(b)** JJAS cumulative rainfall from 1986 to 2015. The black, red and blue lines are the observations and the model simulations-raw and bias-corrected, respectively. The 10th-90th percentile bounds are also shown for the model simulations. The Pearson correlation between observations and model simulations is 0.434, significant at 5% significance level (s.l). **(c)** *same as* (a), for average JJAS temperature. **(d)** *same as* (b), for JJAS average temperature. The Pearson correlation between observations and model simulations is 0.517, significant at 5% significance level (s.l).

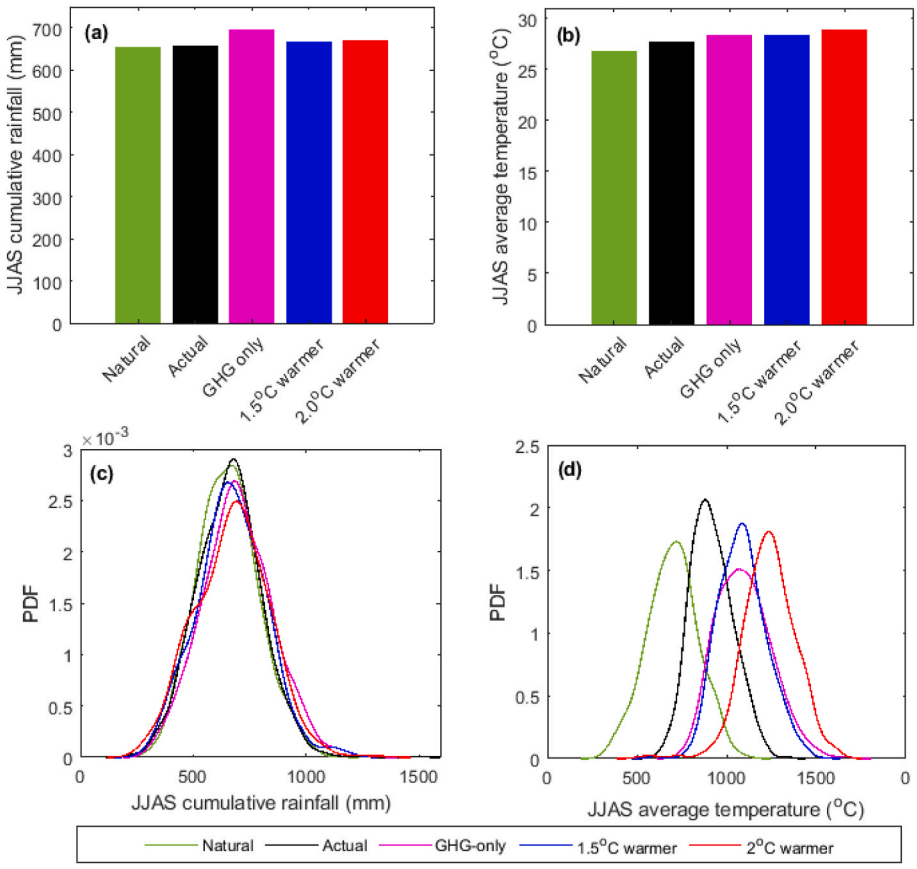

Fig. 6. Long-term averages of **(a)** JJAS cumulative rainfall, and **(b)** Annual average temperature over Marathwada, from the weather@home simulations, for the Natural (green), Actual (black), 1.5 °C (blue) and 2 °C warmer world (red) scenarios. The averaging period for the Natural and Actual scenarios is 2006–2015 while that of the 1.5° and 2 °C warmer (red) worlds is representative 2091–2 100. The probability density function (PDF) estimates for all the four scenarios, are also plotted for **(c)** rainfall, and **(d)** temperature. (For interpretation of the references to colour in this figure legend, the reader is referred to the Web version of this article.)

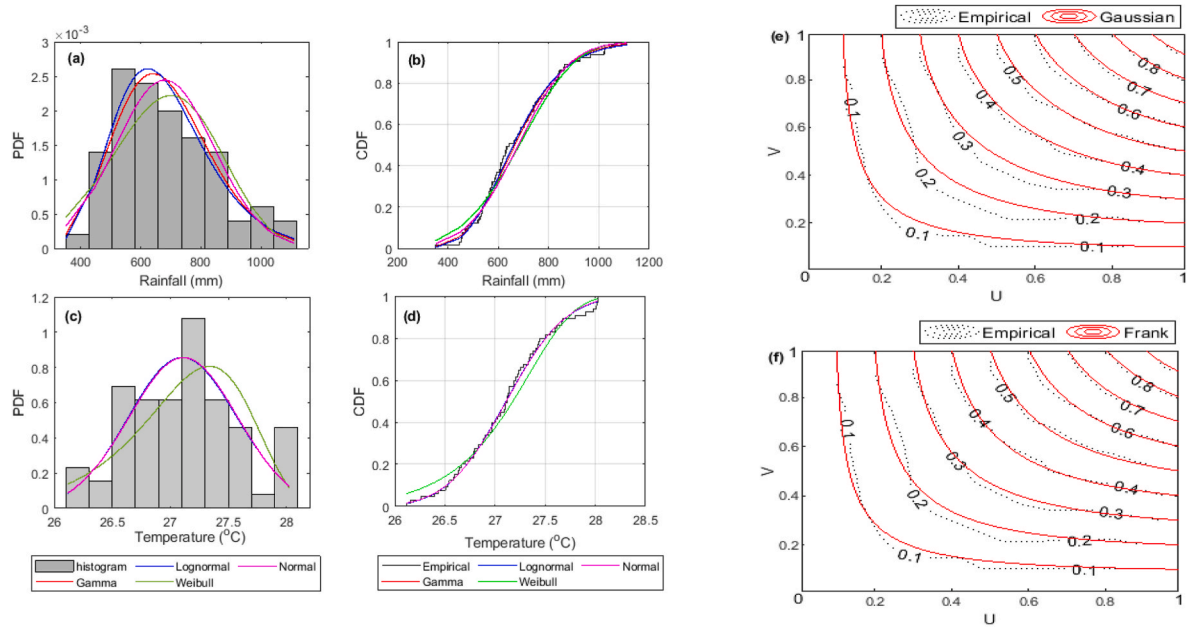

Fig. 7. **(a)** Marginal probability density function (PDF) from selected parametric distributions, and empirical histogram and, **(b)** Marginal CDF from selected parametric distributions and empirical CDF of JJAS cumulative rainfall for 1951–2015 period, over Marathwada. **(c)** same as (a), and **(d)** same as (b), for JJAS average temperature. **(e)** Joint CDF of JJAS cumulative rainfall and JJAS average temperature over Marathwada, from Gaussian copula, along with the empirical CDF. **(f)** same as (e), with the parametric CDF from Frank copula.

events for 20, 50 and 500 years, based on the observed records, for the pre-1985 and post-1985 periods. Fig. 8(b) shows similar return period contours for the five scenarios- Natural, Actual, GHG-only, and the 1.5 °C and 2 °C warmer world, for the 2006–2015 decade. Additionally, the return period contours for the model climatology (from Actual runs for 1986–2015 period) are plotted, for comparing with the estimates based on observed data (Fig. 8(a)). The red pentagram denotes the 2015 hot and dry event. The migration of the observations-based contours to

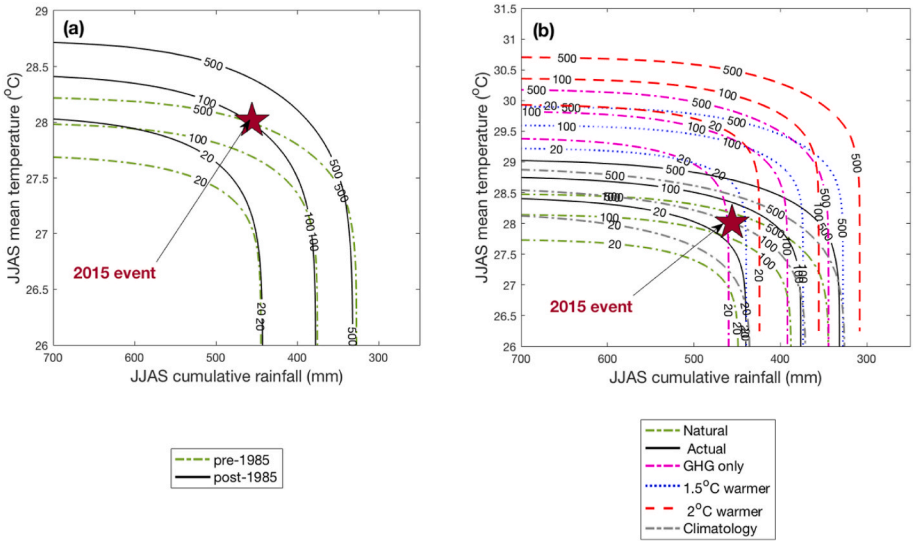

Fig. 8. (a) Multivariate return periods of concurrent temperature and rainfall extremes over Marathwada from observations. Dashed green and solid black isolines show various return levels in pre-1985 and post-1985 period, respectively. The event has return periods of 570 and 110 years, in the pre-1985 and post-1985, respectively. **(b)** *same as (a),* but from the weather@home model simulations for Pre-industrial (green), Actual (black), GHG-only (magenta), 1.5 °C (blue) and 2 °C (red) scenarios, and for the climatology runs (grey). The event has return periods of 262, 38, 22, 15, 12 and 100 years, in the Natural, Actual, GHG-only, 1.5 °C and 2 °C warming scenarios, and the climatology runs, respectively. (For interpretation of the references to colour in this figure legend, the reader is referred to the Web version of this article.)

hotter and drier regimes in the post-1985 period (Fig. 8(a)) indicate that concurrent hot and dry events in Marathwada have intensified and have become more frequent in recent years. Similar inferences can be drawn from the model-based contours too (Fig. 8(b)). The hot and dry events are more frequent and graver in magnitude in the Actual world as compared to the Natural world. Such events are expected to intensify further and become more frequent in the future warmer worlds, and in the absence of aerosols (GHG-only).

The return period of the 2015 hot and dry event from the model climatology runs is 100 years (range: 90–110 years; Table 1(a)). The closeness of the return period estimates between the model climatology (100 years) and the observed post-1985 period (110 years), underlines the reliability of the weather@home model runs for this study. The 2015 event has a high recurrence interval of 262 years (uncertainty range: 216–330 years) in the Natural world without anthropogenic greenhouse gas (GHG) and aerosol emissions, whereas it is a much more frequent 1-in-38 year event (uncertainty range: 1-in-33 year to 1-in-44 year) in the Actual scenario, suggesting that the event is made *more likely* due to anthropogenic climate change ($PR_{Actual/Natural} = 5.3$; best estimate: 7; Fig. 9(a) and Table 1(a)).

For discerning the role of anthropogenic aerosols in the occurrence of hot and dry conditions in Marathwada, we compare the return period of the 2015 hot and dry event in the GHG-only scenario. We note here that the aerosols effects reported in the study are with respect to the reflective (cooling) sulfate aerosols only. HadRM3P does not model absorbing aerosols and associated feedbacks (Massey et al., 2015) which are also important for the Indian region as they tend to warm the atmosphere in contrast to sulfate (Ramanathan et al., 2002; Venkataraman et al., 2005). As far as rainfall is concerned, both absorbing black carbon and sulfate aerosols tend to suppress rainfall as long as temperatures do not change. Concurrent hot and dry events are expected to intensify and become more frequent in the absence of anthropogenic aerosols (Fig. 8 (b)). The 2015 event is found to be more frequent (1-in-22 year) in the GHG-only scenario as compared to Actual due to the warmer atmosphere (Fig. 6(b)), presumably, due to the absence of cooling effect of sulfate aerosols (Huang et al., 2007; Kiehl and Briegleb, 1993; J. F. B. Mitchell et al., 1995; Reader and Boer, 1998). In other words, the presence of aerosols makes the event *exceptionally less likely* in the current climate ($PR_{Actual/GHG-only} = 0.5$; best estimate: 0.6; Fig. 9(a) and Table 1(a)), by abating the warming due to GHG emissions.

Finally, for a prognosis of the expected change in the likelihood of hot and dry events under future warming, we also examine the return period characteristics of the 2015 event under the 1.5 °C and 2 °C warmer world scenarios. The event is expected to become much more frequent, with recurrence intervals of 1-in-15-year (uncertainty range: 1-in-13-year to 1-in-17-year) and 1-in-12-year (uncertainty range: 1-in-10-year to 1-in-14-year) in the 1.5 °C and 2 °C warmer worlds, respectively (Fig. 8(b)). The warming due to the reduction in aerosol emissions (1/3rd of the Actual world concentrations) and increase in GHG emissions under these scenarios (Fig. 6(b)) along with almost no increase in rainfall in the region (Fig. 6(a)) is likely the reason for the increased odds of such event occurring. From Fig. 9(a) and Table 1(a), we can see that the probability of the event is 2.1 times ($PR_{1.5°C/Actual}$; best estimate: 2.6) and 2.8 times ($PR_{2°C/Actual}$ best estimate: 3.3) that of Actual, under 1.5 °C and 2 °C warmer scenarios, respectively, suggesting that the event is expected to become *more likely* under future climate change.

Our findings highlight the need to curb the warming at well-below 1.5 °C above pre-industrial levels, as evidenced by the quintupled risk of the hot-dry event in the factual world as compared to the Natural scenario (Fig. 8 (b); Table 1), along with expected doubling and tripling of risk under future 1.5 °C and 2 °C warming, respectively. However, it is also necessary to compare with univariate estimates based on each of rainfall deficits and temperature exceedances, in order to be able to reconcile our results with existing evidence for the region.

4.5. *Univariate return periods and probability ratios for the 2015 individual rainfall (dry) and temperature (hot) events*

Fig. 10(a) shows the observation-based return period curves for JJAS cumulative rainfall, for the pre-1985 and post-1985 periods. The 2015 event has return periods of 1-in-16 and 1-in-15 year in the pre-1985 and post-1985 periods, respectively, suggesting that the event is not unprecedented upon considering rainfall deficits alone. This observation is qualitatively comparable with the conclusion from an earlier study that examined the characteristics of long-term observed rainfall variability in this region (Kulkarni et al., 2016). The return period curves are also similar in the Actual and Natural scenarios, at 17 years (uncertainty range: 16–19 years) and 15 years (uncertainty range: 13–17 years), respectively (Fig. 10(b)), with probability ratio $PR_{Act/Nat} = 1$ (best estimate: 1.2; Table 1(b) and Fig. 9(b)), which indicates the event may have become at least *less likely* due to climate change. The temperature, on the other hand, shows discernible shifts both in the observed splits and the model-simulated Natural and Actual scenarios. The 2015 hot event, which used to be a 1-in-108 year event in the pre-1985 period, is seen to have become a 1-in-16 year event, post-1985 (Fig. 10(c)). The return period estimates from the Natural and Actual scenarios also show a

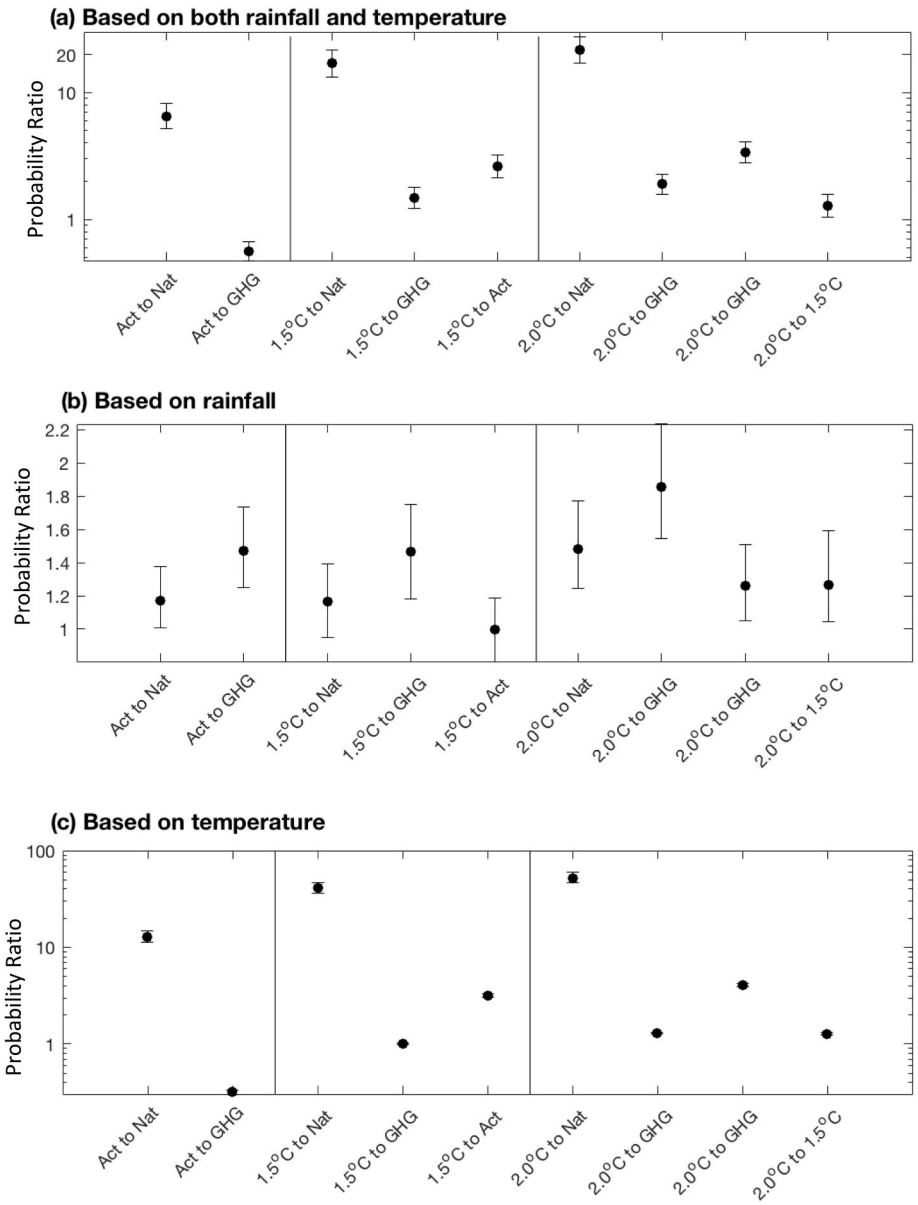

Fig. 9. Probability Ratio (PR) of the 2015 event based on **(a)** both rainfall and temperature, **(b)** for rainfall alone, and **(c)** for temperature alone, for different combinations of model scenarios.

considerable shift from 1-in 55 years to 1-in-4 years (Fig. 10(d)), which translates into a 11-fold increase in risk of anomalously high temperatures due to anthropogenic climate change (Fig. 9(c) and Table 1(c)).

It is difficult to discern the role of aerosols on the regional rainfall, presumably owing to the differing direct and indirect effects of sulfate aerosols (Ackerley et al., 2011; Giorgi et al., 2003). In the absence of aerosols (GHG-only), the rainfall in the region would have been higher (Fig. 6(a)), also reflected as a slight increase in the return period of the 2015 dry event (1-in-22 year) as compared to Actual (Fig. 10(b)). However, this increase is not significant, as highlighted by the probability ratio, $PR_{Actual/GHG-only} = 1.3$ (best estimate: 1.5; Fig. 9(b) and Table 1(b)) which suggests that the risk of the event is *not likely to have altered* even in the absence of aerosols. Unlike rainfall, the absence of cooling aerosols (GHG-only scenario) will have resulted in a warmer atmosphere (Fig. 6(b)). Therefore, the 2015 hot event would have been a very frequent, annual event (Fig. 10(d)).

The return periods of the 2015 dry event under 1.5 °C and 2 °C warmer worlds are also close to the estimates from the other scenarios (Fig. 10(b)), at 15 years (uncertainty range: 13–17 years) and 12 years (uncertainty range: 10–14 years), respectively. However, this marginal to no change in the recurrence characteristics of rainfall in the different model scenarios cannot be conclusively attributed to the absence of climate change signal; rather, it is an indication that the climate signals may be confounded due to the high variability in the Indian Summer Monsoon Rainfall (Singh 2016; Tebaldi et al., 2011). The 2015 hot event is expected to become an annual event under future warming, likely due to the reduction in aerosols (1/3rd of concentration in Actual; Supp S1) and change in GHG concentrations. It may be noted that our experimental set-up is designed to isolate the climate change signal from natural variability due to other global SST patterns (Guillod et al., 2017), on account of the scenarios being forced with observed SST patterns that are shifted to the respective warming levels (see Supp. S1; Table S1). Therefore, for any given year, such as 2015, the influence of ENSO is the same across all scenarios. This influence gets smoothed on considering a range of years (2006–2015). This difference is also reflected in the probabilities and therefore the PRs, as shown in Table S3 for the 2015-only ensembles as compared to the estimates based on the

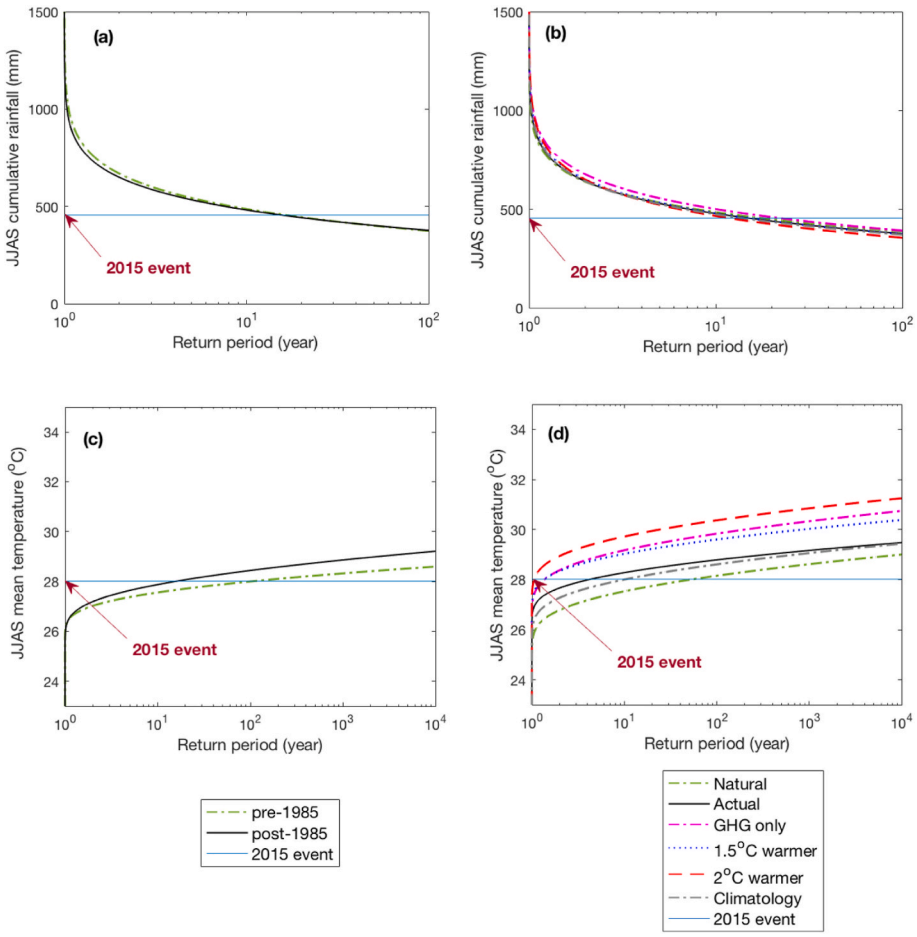

Fig. 10. **(a)** Univariate return periods of rainfall over Marathwada from observations. Dashed green and solid black isolines show various return levels in pre-1985 and post-1985 period, respectively. The event has return periods of 16 and 15 years, in the pre-1985 and post-1985, respectively. **(b)** *same as (a),* but from the weather@home model simulations for Pre-industrial (green), Actual (black), GHG-only (magenta), 1.5 °C (blue) and 2 °C (red) scenarios, and for the climatology runs (grey). The event has return periods of 17, 15, 22, 15, 12 and 14 years, in the Natural, Actual, GHG-only, 1.5 °C and 2 °C warming scenarios, and the climatology runs,respectively. **(c)** *same as* (a), for temperature. The event has return periods of 108 and 16 years, in the pre-1985 and post-1985, respectively. **(d)** *same as (b),* for temperature. The event has return periods of 55, 4, 1, 1 and 1 and 10 year(s), in the Natural, Actual, GHG-only, 1.5 °C and 2 °C warming scenarios, and the climatology runs, respectively. (For interpretation of the references to colour in this figure legend, the reader is referred to the Web version of this article.)

2006-15 ensemble in Table 1.

Overall, it is interesting to note that for either of the observed periods and for all of the climate scenarios, the 2015 rainfall deficit itself is not unprecedented (Fig. 10(a–b)); however, the corresponding hot-dry event is rare, and poised to become more frequent under warming (Fig. 8(a–b)). For instance, the return period of the 2015 rainfall event is only 15 years for the post-1985 period, while the corresponding hot-dry event is rare, with a return period of 110 years. In a nutshell, the findings from this study emphasize the role of temperature in compounding droughts in the region by causing concurrent hot-dry conditions, and provide a pragmatic attribution (with *medium confidence*, as discussed in Section 4.2) of the 2015 event to anthropogenic climate change.

5. Concluding remarks

The 2015 drought in Marathwada was a catastrophic event, potentially amplified by the compounded role of anomalously high temperature and rainfall deficits, and resulting in large loss to agriculture and lives (Gruère and Sengupta 2011; Sridhar 2006). In this study, we carried out a PEA analysis of this hot and dry event in a first-of-its-kind copula-based multivariate attribution framework. On comparing the return period of the 2015 hot-dry event against the traditional univariate return period of the 2015 rainfall, in both observed records and model scenarios from the weather@home climate model simulations, we found that the rainfall event was not unprecedented, whereas the compounded hot and dry condition was rare.

The two important findings from this study are as follows - (i) it is *more likely* that the 2015 hot and dry event can almost entirely be attributed to anthropogenic emissions ($PR_{Actual/Natural} = 5.3$), and (ii) such an event is also *likely* to occur under future 1.5 °C and 2 °C warmer worlds with expected doubling and tripling of risks, respectively, as compared to the factual world. For an agriculture-driven economy such as that of India, these results bear strong implications and highlight the importance of a multivariate analysis to study compound extreme events. Therefore, it is imperative to focus on strategies that strive to limit warming in the region well below 1.5 °C, recognizing the plausible impacts in terms of agricultural loss and mortality caused by increased future occurrences of such events. Furthermore, the multiplied change in risk of droughts in Marathwada under future warming scenarios also seem to suggest an unequal and unjust ramification of global climate change in vulnerable regions of the world.

An important caveat in this study is that we have not used multiple model ensembles. However, the model evaluations against observed data and the return period estimates from the observed and model climatologies are found to match closely, thus making the evidence robust. Further, an in-depth analysis of the large-scale teleconnections that drive ISMR (e.g., Cherchi and Navarra, 2013) and the interactions of meteorological and hydrologic variables, atmospheric chemistry at regional scales and the local feedback from irrigation (e.g., Ambika and Mishra, 2021) on the associated risks can form a part of future studies in this area.

The multivariate approach presented in this study can also be modified for estimating the conditional relationship between the two variables (Hao et al., 2018). For example, the conditional distribution of rainfall given an antecedent JJAS average temperature can be used to estimate the impact of high temperatures on droughts under different scenarios, which is a reflection of the soil moisture-climate interactions (Seneviratne et al., 2010). Further, our framework is generic and can be applied to include other relevant variables such as soil moisture and

groundwater information. Finally, an end-to-end framework (Mitchell et al., 2016; Schaller et al., 2016) that links attribution analyses to impacts such as crop loss or (indirect) farmer suicides can provide additional guidance on how to mitigate risks.

CRediT authorship contribution statement

Mariam Zachariah: Conceptualization, Methodology, Software, Validation, Formal analysis, Data curation, Writing – original draft, Writing – review & editing, Visualization. **Savitri Kumari:** Methodology, Software, Validation, Formal analysis, Data curation, Writing – original draft, Writing – review & editing, Visualization. **Arpita Mondal:** Conceptualization, Methodology, Formal analysis, Data curation, Writing – original draft, Writing – review & editing, Visualization, Supervision, Project administration, Funding acquisition. **Karsten Haustein:** Methodology, Software, Validation, Formal analysis, Data curation, Writing – original draft, Writing – review & editing, Visualization, Supervision. **Friederike E.L. Otto:** Methodology, Software, Validation, Formal analysis, Data curation, Writing – original draft, Writing – review & editing, Visualization, Supervision, Project administration, Funding acquisition.

Declaration of competing interest

The authors declare that they have no known competing financial interests or personal relationships that could have appeared to influence the work reported in this paper.

Data availability

Data will be made available on request.

Acknowledgments and Data

The authors would like to thank India Meteorological Department for making the observed rainfall and temperature data publically available at http://www.imdpune.gov.in/Clim_Pred_LRF_New/Grided_Data_Download.html. The raw data for the weather@home simulations used in this study, can be regenerated using the CPDN portal (https://www.cpdn.org). We thank Amir AghaKouchak for helpful discussions. We would also like to thank the volunteers who have donated their computing time to weather@home. AM and SK would like to thank DST-UKIERI for financial support through sponsored project DST/INT/UK/P-135/2016. MZ is supported by the Industrial Research & Consultancy Centre Fellowship, IIT Bombay through sponsored project 15IRCCSG036.

Appendix A. Supplementary data

Supplementary data to this article can be found online at https://doi.org/10.1016/j.wace.2022.100546.

References

Ackerley, D., Booth, B.B.B., Knight, S.H.E., Highwood, E.J., Frame, D.J., Allen, M.R., Rowell, D.P., 2011. Sensitivity of twentieth-century Sahel rainfall to sulfate aerosol and CO2 forcing. J. Clim. 24 (19), 4999–5014.

AghaKouchak, A., Cheng, L., Mazdiyasni, O., Farahmand, A., 2014. Global warming and changes in risk of concurrent climate extremes: insights from the 2014 California drought. Geophys. Res. Lett. 41 (24), 8847–8852.

Akaike, H. (1386). "A new look at the statistical model identification." *IEEE Transactions of Automatic Control*, AC-19(6), 716–723.

Allen, M.R., Dube, O.P., Solecki, W., Aragón-Durand, F., Cramer, W., Humphreys, S., Kainuma, M., Kala, J., Mahowald, N., Mulugetta, Y., Perez, R., Wairiu, M., Zickfeld, K., 2018. Framing and Context. In: Masson-Delmotte, V., Zhai, P., Pörtner, H.-O., Roberts, D., Skea, J., Shukla, P.R., Pirani, A., Moufouma-Okia, W., Péan, C., Pidcock, R., Connors, S., Matthews, J.B.R., Chen, Y., Zhou, X., Gomis, M.I., Lonnoy, E., Maycock, T., Tignor, M., Waterfiel, T. (Eds.), Global Warming of 1.5°C. An IPCC Special Report on the impacts of global warming of 1.5°C above pre-industrial levels and related global greenhouse gas emission pathways, in the context of strengthening the global response to the threat of climate change, sustainable development, and efforts to eradicate poverty. Cambridge University Press, Cambridge, UK and New York, NY, USA, pp. 49–92.

Ambika, A.K., Mishra, V., 2021. Modulation of compound extremes of low soil moisture and high vapor pressure deficit by irrigation in India. J. Geophys. Res. Atmos. 126 (7).

Bhavani, P., Chakravarthi, V., Roy, P.S., Joshi, P.K., Chandrasekar, K., 2017. Long-term agricultural performance and climate variability for drought assessment: a regional study from Telangana and Andhra Pradesh states, India. Geomatics, Nat. Hazards Risk 8 (2), 822–840.

Bollasina, M.A., Ming, Y., Ramaswamy, V., 2011. Anthropogenic aerosols and the weakening of the South Asian summer monsoon. Science 334 (6055), 502–505.

Bozdogan, H., 2000. Akaike's information criterion and recent developments in information complexity. J. Math. Psychol. 44 (1), 62–91.

Cannon, A.J., 2016. Multivariate bias correction of climate model output: matching marginal distributions and intervariable dependence structure. J. Clim. 29 (19), 7045–7064.

Carleton, T.A., 2017. Crop-damaging temperatures increase suicide rates in India. Proc. Natl. Acad. Sci. USA 114 (33), 8746–8751.

Chaudhary, S., Dhanya, C.T., Vinnarasi, R., 2017. Dry and wet spell variability during monsoon in gauge-based gridded daily precipitation datasets over India. J. Hydrol. 546, 204–218.

Cherchi, A., Navarra, A., 2013. Influence of ENSO and of the Indian Ocean Dipole on the Indian summer monsoon variability. Clim. Dynam. 41 (1), 81–103.

Chiang, F., Greve, P., Mazdiyasni, O., Wada, Y., AghaKouchak, A., 2021. A multivariate conditional probability ratio framework for the detection and attribution of compound climate extremes. Geophys. Res. Lett. 48 (15), 6.

Chiang, F., Mazdiyasni, O., AghaKouchak, A., 2018. Amplified warming of droughts in southern United States in observations and model simulations. Sci. Adv. 4 (8), eaat2380.

Cong, R.-G., Brady, M., 2012. The interdependence between rainfall and temperature: copula analyses. Sci. World J. 2012 (5106), 1–11.

Deulgaonkar, A., Joshi, A., 2016. Deaths Multiply in Parched Marathwada ([Blog post]).

Diffenbaugh, N.S., Swain, D.L., Touma, D., 2015. Anthropogenic warming has increased drought risk in California. Proc. Natl. Acad. Sci. USA 112 (13), 3931–3936.

Donlon, C.J., Martin, M., Stark, J., Roberts-Jones, J., Fiedler, E., Wimmer, W., 2012. The operational Sea Surface temperature and Sea Ice analysis (OSTIA) system. Rem. Sens. Environ. 116, 140–158.

Duncan, J.M.A., Saikia, S.D., Gupta, N., Biggs, E.M., 2016. Observing climate impacts on tea yield in Assam, India. Appl. Geogr. 77, 64–71.

Fernandes, S., 2016. Marathwada Drought Man-Made , Not Caused by Climate Change : Study. Hindustan Times, Mumbai.

Galmarini, S., Cannon, A.J., Ceglar, A., Christensen, O.B., de Noblet-Ducoudré, N., Dentener, F., Doblas-Reyes, F.J., Dosio, A., Gutierrez, J.M., Iturbide, M., Jury, M., Lange, S., Loukos, H., Maiorano, A., Maraun, D., McGinnis, S., Nikulin, G., Riccio, A., Sanchez, E., Solazzo, E., Toreti, A., Vrac, M., Zampieri, M., 2019. Adjusting climate model bias for agricultural impact assessment: how to cut the mustard. Climate Services 13 (June 2018), 65–69. Elsevier.

Gangan, S.P., 2016. Marathwada Records More Farmer Suicides than Even Vidarbha. Hindustan Times, Mumbai.

Ghatak, D., Zaitchik, B., Hain, C., Anderson, M., 2017. The role of local heating in the 2015 Indian Heat Wave. Sci. Rep. 7 (1), 7707.

Ghatge, S., 2016. Marathwada's Drought: How Climate Change Has Destroyed Agriculture and Ruined Farmers ([Blog post]).

Ghosh, S., Vittal, H., Sharma, T., Karmakar, S., Kasiviswanathan, K.S., Dhanesh, Y., Sudheer, K.P., Gunthe, S.S., 2016. Indian summer monsoon rainfall: implications of contrasting trends in the spatial variability of means and extremes. In: Li, C. (Ed.), PLoS One 11 (7), e0158670.

Giorgi, F., Bi, X., Qian, Y., 2003. Indirect vs. direct effects of anthropogenic sulfate on the climate of east Asia as simulated with a regional coupled climate-chemistry/aerosol model. Climatic Change 58 (3), 345–376.

Goyal, R.K., 2004. Sensitivity of evapotranspiration to global warming: a case study of arid zone of Rajasthan (India). Agric. Water Manag. 69 (1), 1–11.

Gringorten, I.I., 1963. A plotting rule for extreme probability paper. J. Geophys. Res. 68 (3), 813–814.

Gruère, G., Sengupta, D., 2011. Bt Cotton and farmer suicides in India: an evidence-based assessment. J. Dev. Stud. 47 (2), 316–337.

Guhathakurta, P., Rajeevan, M., 2008. Trends in the rainfall pattern over India. Int. J. Climatol. 28 (11), 1453–1469.

Guillod, B.P., Jones, R.G., Bowery, A., Haustein, K., Massey, N.R., Mitchell, D.M., Otto, F. E.L., Sparrow, S.N., Uhe, P., Wallom, D.C.H., Wilson, S., Allen, M.R., 2017. weather@home 2: validation of an improved global–regional climate modelling system. Geosci. Model Dev. (GMD) 10 (5), 1849–1872.

Hansen, J., Sato, M., Ruedy, R., 2012. Perception of climate change. Proc. Natl. Acad. Sci. USA 109 (37), E2415–E2423.

Hao, Z., Singh, V., Hao, F., 2018. Compound extremes in hydroclimatology: a review. Water 10 (6), 718.

Hao, Z., Singh, V.P., 2020. Compound events under global warming: a dependence perspective. J. Hydrol. Eng. 25 (9), 03120001.

Huang, Y., Chameides, W.L., Dickinson, R.E., 2007. Direct and indirect effects of anthropogenic aerosols on regional precipitation over east Asia. J. Geophys. Res. 112 (D3), D03212.

IMD (India Meteorological Department), 2016. Annual Climate Summary - 2015. Pune.

Jain, B., 2016. Rs 4,100 Crore Maharashtra Crop Loss Claims Tip of Iceberg ? The Times of India, Mumbai.

Katzenberger, A., Schewe, J., Pongratz, J., Levermann, A., 2021. Robust increase of Indian monsoon rainfall and its variability under future warming in CMIP6 models. Earth Syst. Dynamic. 12 (2), 367–386.
Kelkar, R.R., Sreejith, O.P., 2020. Meteorological sub-divisions of India and their geopolitical evolution from 1875 to 2020. Mausam 71 (4), 571–584.
Kiehl, J.T., Briegleb, B.P., 1993. The relative roles of sulfate aerosols and greenhouse gases in climate forcing. Science 260 (5106), 311–314.
Kolmogorov, A.N., 1933. Sulla determinazione empirica di una legge di distribuzione. Giornale Instituto Italiano Attuari 4, 83–91.
Kripalani, R.H., Kulkarni, A., 1997. Climatic impact of El Niño/La Niña on the Indian monsoon: a new perspective. Weather 52 (2), 39–46.
Kulkarni, A., Gadgil, S., Patwardhan, S., 2016. Monsoon variability, the 2015 Marathwada drought and rainfed agriculture. Curr. Sci. 111 (7), 1182.
Kumar, K.K., Rajagopalan, B., Hoerling, M., Bates, G., Cane, M., 2006. Unraveling the mystery of Indian monsoon failure during El Nino. Science 314 (5796), 115–119.
Kumar, R., Mishra, V., Buzan, J., Kumar, R., Shindell, D., Huber, M., 2017. Dominant control of agriculture and irrigation on urban heat island in India. Sci. Rep. 7 (1), 14054. Springer US.
Kumari, S., Haustein, K., Javid, H., Burton, C., Allen, M.R., Paltan, H., Dadson, S., Otto, F. E.L., 2019. Return period of extreme rainfall substantially decreases under 1.5 °C and 2.0 °C warming: a case study for Uttarakhand, India. Environ. Res. Lett. 14 (4), 044033.
Lewis, S.C., King, A.D., Perkins-Kirkpatrick, S.E., Wehner, M.F., 2019. Toward calibrated language for effectively communicating the results of extreme event attribution studies. Earth's Future 7 (9), 1020–1026.
Li, D., Feng, J., Dosio, A., Qi, J., Xu, Z., Yin, B., 2020. Historical evaluation and future projections of 100-m wind energy potentials over CORDEX-East Asia. J. Geophys. Res. Atmos. 125 (15).
Li, H., Sheffield, J., Wood, E.F., 2010. Bias correction of monthly precipitation and temperature fields from Intergovernmental Panel on Climate Change AR4 models using equidistant quantile matching. J. Geophys. Res. 115 (D10), D10101.
Lott, F.C., Christidis, N., Stott, P.A., 2013. Can the 2011 East African drought be attributed to human-induced climate change? Geophys. Res. Lett. 40 (6), 1177–1181.
Massey, F.J., 1951. The Kolmogorov-Smirnov test for goodness of fit. J. Am. Stat. Assoc. 46 (253), 68–78.
Massey, N., Jones, R., Otto, F.E.L., Aina, T., Wilson, S., Murphy, J.M., Hassell, D., Yamazaki, Y.H., Allen, M.R., 2015. weather@home—development and validation of a very large ensemble modelling system for probabilistic event attribution. Q. J. R. Meteorol. Soc. 141 (690), 1528–1545. John Wiley & Sons, Ltd.
Mazdiyasni, O., AghaKouchak, A., Davis, S.J., Madadgar, S., Mehran, A., Ragno, E., Sadegh, M., Sengupta, A., Ghosh, S., Dhanya, C.T., Niknejad, M., 2017. Increasing probability of mortality during Indian heat waves. Sci. Adv. 3 (6), e1700066.
Mishra, V., Shah, R., Thrasher, B., 2014. Soil moisture droughts under the retrospective and projected climate in India. J. Hydrometeorol. 15 (6), 2267–2292.
Mishra, V., Thirumalai, K., Singh, D., Aadhar, S., 2020. Future exacerbation of hot and dry summer monsoon extremes in India. NPJ Climate Atmosphere Sci. 3 (1), 10. Springer US.
Mishra, V., Tiwari, A.D., Aadhar, S., Shah, R., Xiao, M., Pai, D.S., Lettenmaier, D., 2019. Drought and famine in India, 1870–2016. Geophys. Res. Lett. 46 (4), 2075–2083.
Mitchell, D., AchutaRao, K., Allen, M., Bethke, I., Beyerle, U., Ciavarella, A., Zaaboul, R., 2017. Half a degree additional warming, prognosis and projected impacts (HAPPI): background and experimental design. Geosci. Model Dev. 10 (2), 571–583.
Mitchell, D., Heaviside, C., Vardoulakis, S., Huntingford, C., Masato, G., P Guillod, B., Frumhoff, P., Bowery, A., Wallom, D., Allen, M., 2016. Attributing human mortality during extreme heat waves to anthropogenic climate change. Environ. Res. Lett. 11 (7), 074006.
Mitchell, J.F.B., Johns, T.C., Gregory, J.M., Tett, S.F.B., 1995. Climate response to increasing levels of greenhouse gases and sulphate aerosols. Nature 376 (6540), 501–504.
Mujumdar, M., Gnanaseelan, C., Rajeevan, M. (Eds.), 2015. A Research Report on the 2015 Southwest Monsoon. Pune.
Myung, I.J., 2003. Tutorial on maximum likelihood estimation. J. Math. Psychol. 47 (1), 90–100.
NCRB (National Crime Records Bureau), 2016. Accidental Deaths & Suicides in India 2015 (New Delhi).
Nelsen, R.B., 2006. An Introduction to Copulas. Springer Series in Statistics. Springer, New York, New York, NY.
New, M., Hulme, M., Jones, P., 2000. Representing twentieth-century space–time climate variability. Part II: development of 1901–96 monthly grids of terrestrial surface climate. J. Clim. 13 (13), 2217–2238.
Nicholls, N., 2004. The changing nature of Australian droughts. Climatic Change 63 (3), 323–336.
UNFCCC (United Nations Framework Convention on Climate Change), 2016. In: Paris Agreement." Report of the Conference of the Parties on its twenty-first session, held in Paris from 30 November to 13 December 2015 Addendum Part two: Action taken by the Conference of the Parties at its twenty-first session FCCC/CP/2015/10/Add.1, pp. 21–36.
van Oldenborgh, G.J., Philip, S., Kew, S., van Weele, M., Uhe, P., Otto, F., Singh, R., Pai, I., Cullen, H., AchutaRao, K., 2018. Extreme heat in India and anthropogenic climate change. Nat. Hazards Earth Syst. Sci. 18 (1), 365–381.
Otto, F.E.L., Massey, N., van Oldenborgh, G.J., Jones, R.G., Allen, M.R., 2012. Reconciling two approaches to attribution of the 2010 Russian heat wave. Geophys. Res. Lett. 39 (4), L04702.
Pai, D.S., Sridhar, L., Rajeevan, M., Sreejith, O.P., Satbhai, N.S., Mukhopadhyay, B., 2014. Development of a new high spatial resolution (0.25° × 0.25°) long period (1901-2010) daily gridded rainfall data set over India and its comparison with existing data sets over the region. Mausam 65 (1), 1–18.
Pall, P., Aina, T., Stone, D.A., Stott, P.A., Nozawa, T., Hilberts, A.G.J., Lohmann, D., Allen, M.R., 2011. Anthropogenic greenhouse gas contribution to flood risk in England and Wales in autumn 2000. Nature 470 (7334), 382–385.
Panda, D.K., AghaKouchak, A., Ambast, S.K., 2017. Increasing heat waves and warm spells in India, observed from a multiaspect framework. J. Geophys. Res. Atmos. 122 (7), 3837–3858.
Pandey, P.K., Das, L., Jhajharia, D., Pandey, V., 2018. Modelling of interdependence between rainfall and temperature using copula. Model Earth Syst. Environ. 4 (2), 867–879. Springer International Publishing.
Parida, Y., Dash, D.P., Bhardwaj, P., Chowdhury, J.R., 2018. Effects of drought and flood on farmer suicides in Indian states: an empirical analysis, 2. In: Economics of Disasters and Climate Change, Economics of Disasters and Climate Change, 2, pp. 159–180.
Paul, S., Ghosh, S., Oglesby, R., Pathak, A., Chandrasekharan, A., Ramsankaran, R., 2016. Weakening of Indian Summer Monsoon rainfall due to changes in land use land cover. Sci. Rep. 6 (1), 32177.
Philip, S., Kew, S.F., Jan van Oldenborgh, G., Otto, F., O'Keefe, S., Haustein, K., King, A., Zegeye, A., Eshetu, Z., Hailemariam, K., Singh, R., Jjemba, E., Funk, C., Cullen, H., 2018. Attribution analysis of the Ethiopian drought of 2015. J. Clim. 31 (6), 2465–2486.
Philip, S., Kew, S., van Oldenborgh, G.J., Otto, F., Vautard, R., van der Wiel, K., King, A., Lott, F., Arrighi, J., Singh, R., van Aalst, M., 2020. A protocol for probabilistic extreme event attribution analyses. Adv. Stats. Climatol. Meteorol. Oceanograph. 6 (2), 177–203.
Preethi, B., Ramya, R., Patwardhan, S.K., Mujumdar, M., Kripalani, R.H., 2019. Variability of Indian summer monsoon droughts in CMIP5 climate models. Clim. Dynam. 53 (3–4), 1937–1962.
Purohit, M.K., Kaur, S., 2017. Rainfall Statistics of India - 2016 (New Delhi).
Ramanathan, V., Crutzen, P.J., Mitra, A.P., Sikka, D., 2002. The Indian ocean experiment and the Asian brown cloud. Curr. Sci. 83 (8), 947–955.
Ratnam, J.V., Behera, S.K., Ratna, S.B., Rajeevan, M., Yamagata, T., 2016. Anatomy of Indian heatwaves. Sci. Rep. 6 (1), 24395.
Reader, M.C., Boer, G.J., 1998. The modification of greenhouse gas warming by the direct effect of sulphate aerosols. Clim. Dynam. 14 (7–8), 593–607.
Roberts, M.J., Schlenker, W., Eyer, J., 2013. Agronomic weather measures in econometric models of crop yield with implications for climate change. Am. J. Agric. Econ. 95 (2), 236–243.
Roxy, M.K., Ritika, K., Terray, P., Murtugudde, R., Ashok, K., Goswami, B.N., 2015. Drying of Indian subcontinent by rapid Indian Ocean warming and a weakening land-sea thermal gradient. Nat. Commun. 6 (1), 7423.
Sarhadi, A., Ausín, M.C., Wiper, M.P., Touma, D., Diffenbaugh, N.S., 2018. Multidimensional risk in a nonstationary climate: joint probability of increasingly severe warm and dry conditions. Sci. Adv. 4 (11), eaau3487.
Schaller, N., Kay, A.L., Lamb, R., Massey, N.R., van Oldenborgh, G.J., Otto, F.E.L., Sparrow, S.N., Vautard, R., Yiou, P., Ashpole, I., Bowery, A., Crooks, S.M., Haustein, K., Huntingford, C., Ingram, W.J., Jones, R.G., Legg, T., Miller, J., Skeggs, J., Wallom, D., Weisheimer, A., Wilson, S., Stott, P.A., Allen, M.R., 2016. Human influence on climate in the 2014 southern England winter floods and their impacts. Nat. Clim. Change 6 (6), 627–634.
Seetharaman, G., 2017. Why Drought-Prone Marathwada Needs to Look beyond the Immediate Monsoons. The Economic Times.
Seneviratne, S.I., Corti, T., Davin, E.L., Hirschi, M., Jaeger, E.B., Lehner, I., Orlowsky, B., Teuling, A.J., 2010. Investigating soil moisture–climate interactions in a changing climate: a review. Earth Sci. Rev. 99 (3–4), 125–161.
Serinaldi, F., 2016. Can we tell more than we can know? The limits of bivariate drought analyses in the United States. Stoch. Environ. Res. Risk Assess. 30 (6), 1691–1704. Springer Berlin Heidelberg.
Sharma, S., Mujumdar, P., 2017. Increasing frequency and spatial extent of concurrent meteorological droughts and heatwaves in India. Sci. Rep. 7 (1), 15582. Springer US.
Shepard, D., 1968. A two-dimensional interpolation function for irregularly-spaced data. In: Proceedings of the 1968 23rd ACM National Conference on. ACM Press, New York, New York, USA, pp. 517–524.
Shepard, D.S., 1984. Computer mapping: the SYMAP interpolation algorithm. Spatial Stats. Model. 133–145. Springer Netherlands, Dordrecht.
Singh, D., 2016. Tug of war on rainfall changes. Nat. Clim. Change 6 (1), 20–22.
Singh, D., Tsiang, M., Rajaratnam, B., Diffenbaugh, N.S., 2014. Observed changes in extreme wet and dry spells during the South Asian summer monsoon season. Nat. Clim. Change 4 (6), 456–461.
Sippel, S., Otto, F.E.L., 2014. Beyond climatological extremes - assessing how the odds of hydrometeorological extreme events in South-East Europe change in a warming climate. Climatic Change 125 (3–4), 381–398.
Smirnov, N., 1948. Table for estimating the goodness of fit of empirical distributions. Ann. Math. Stat. 19 (2), 279–281.
Soora, N.K., Aggarwal, P.K., Saxena, R., Rani, S., Jain, S., Chauhan, N., 2013. An assessment of regional vulnerability of rice to climate change in India. Climatic Change 118 (3–4), 683–699.
Sridhar, V., 2006. Why do farmers commit suicide. Econ. Polit. Wkly. 41 (16), 1559–1565.
Srivastava, A.K., Rajeevan, M., Kshirsagar, S.R., 2009. Development of a high resolution daily gridded temperature data set (1969-2005) for the Indian region. Atmos. Sci. Lett. 10 (October) (n/a-n/a).
Stone, D.A., Allen, M.R., 2005. The end-to-end qttribution problem: from emissions to impacts. Climatic Change 71 (3), 303–318.

Stott, P.A., Stone, D.A., Allen, M.R., 2004. Human contribution to the European heatwave of 2003. Nature 432 (7017), 610–614. Macmillian Magazines Ltd.
Tam, B.Y., Szeto, K., Bonsal, B., Flato, G., Cannon, A.J., Rong, R., 2019. CMIP5 drought projections in Canada based on the standardized precipitation evapotranspiration index. Can. Water Resour. J./Revue canadienne des ressources hydriques 44 (1), 90–107.
Tebaldi, C., Arblaster, J.M., Knutti, R., 2011. Mapping model agreement on future climate projections. Geophys. Res. Lett. 38 (23) (n/a-n/a).
Thompson, A., Otto, F.E.L., 2015. Ethical and normative implications of weather event attribution for policy discussions concerning loss and damage. Climatic Change 133 (3), 439–451.
Uhe, P., Philip, S., Kew, S., Shah, K., Kimutai, J., Mwangi, E., van Oldenborgh, G.J., Singh, R., Arrighi, J., Jjemba, E., Cullen, H., Otto, F., 2018. Attributing drivers of the 2016 Kenyan drought. Int. J. Climatol. 38 (December 2017), e554–e568.
Venkataraman, C., Habib, G., Eiguren-Fernandez, A., Miguel, A.H., Friedlander, S.K., 2005. Residential biofuels in South Asia: carbonaceous aerosol emissions and climate impacts. Science 307 (5714), 1454–1456.
Vinnarasi, R., Dhanya, C.T., 2016. Changing characteristics of extreme wet and dry spells of Indian monsoon rainfall. J. Geophys. Res. Atmos. 121 (5), 2146–2160.
Vyas, S., 2016. Centre steps in with special aid to help drought-hit areas. The Hindu. https://www.thehindu.com/news/cities/mumbai/centre-steps-in-with-special-aid-to-help-droughthit-areas-in-maharashtra/article8554596.ece.
Wazneh, H., Arain, M.A., Coulibaly, P., Gachon, P., 2020. Evaluating the dependence between temperature and precipitation to better estimate the risks of concurrent extreme weather events. In: Rigo, T. (Ed.), Adv. Meteorol. 2020, 1–16.
Wehner, M., Stone, D., Krishnan, H., AchutaRao, K., Castillo, F., 2016. The deadly combination of heat and humidity in India and Pakistan in summer 2015. Bull. Am. Meteorol. Soc. 97 (12), S81–S86.
Willmott, C.J., Rowe, C.M., Philpot, W.D., 1985. Small-Scale climate maps: a sensitivity Analysis of some common assumptions associated with grid-point interpolation and contouring. Am. Cartogr. 12 (1), 5–16.
Wu, J., Han, Z., Li, R., Xu, Y., Shi, Y., 2021. Changes of extreme climate events and related risk exposures in Huang-Huai-Hai river basin under 1.5–2°C global warming targets based on high resolution combined dynamical and statistical downscaling dataset. Int. J. Climatol. 41 (2), 1383–1401.
Yue, S., 2001. A bivariate extreme value distribution applied to flood frequency analysis. Nord. Hydrol 32 (1), 49–64.
Zscheischler, J., Seneviratne, S.I., 2017. Dependence of drivers affects risks associated with compound events. Sci. Adv. 3 (6), e1700263.
Zscheischler, J., Westra, S., van den Hurk, B.J.J.M., Seneviratne, S.I., Ward, P.J., Pitman, A., AghaKouchak, A., Bresch, D.N., Leonard, M., Wahl, T., Zhang, X., 2018. Future climate risk from compound events. Nat. Clim. Change 8 (6), 469–477. Springer US.